Progress In Electromagnetics Research Letters, Vol. 12, 11–20, 2009

NOVEL MICROSTRIP BANDPASS FILTERS USING DIRECT-COUPLED TRIANGULAR STEPPED-IMPEDANCE RESONATORS FOR SPURIOUS SUPPRESSION

K.-S. Chin and D.-J. Chen

Chang Gung University
Taoyuan 333, Taiwan, R.O.C.

Abstract—This paper presents a novel spurious suppressed bandpass filter designed with triangular stepped-impedance resonators. The proposed resonators are folded for a triangular schematic, which creates two transmission zeros. By varying the line width of resonators, one of the zeros is tuned to suppress the first and second spurious responses, and the other is used to improve skirt selectivity. The current study analytically derives explicit design equations and fabricates a three-pole Chebyshev bandpass filter centered at 1.5 GHz based on the direct-coupled structure. The experimental results show spurious suppression improvement more than 20 dB up to $5.6f_0$.

1. INTRODUCTION

Designers widely use half-wavelength hairpin resonators to construct microwave and wireless bandpass filters. The hairpin resonator has attractive features because its structure suffices for compact size and easy fabrication [1–6]. Since the length of resonators is $\lambda/2$, such filters have a spurious passband at nf_0, where f_0 is the operating frequency. However, bandpass filters with spurious suppressed responses and good skirt rate are always required to improve frequency selectivity for modern communication systems.

Researches have presented numerous effective approaches for spurious suppression. Slow-wave resonators [7] push spurious resonances to higher frequencies to extend the upper stopband. Defected ground structures are utilized to provide attenuation poles to yield a wide stopband [8]. The lowpass or bandstop circuits can be incorporated into bandpass filters to suppress unwanted spurious

Corresponding author: K.-S. Chin (kschin@mail.cgu.edu.tw).

passbands [9]. Wu et al. [10] adopted the semi-lumped parallel-resonance structure and capacitive microstrip-CPW broadside-coupled structure [11] to generate transmission zeros to suppress spurious responses. In [12], a novel open-loop stepped-impedance resonator was developed to create two transmission zeros in the upper stopband and thus provide a sharp transition band and multi-spurious suppression.

This paper utilizes triangular stepped-impedance resonators to synthesize microstrip bandpass filters based on the direct-coupled-resonator structure. The proposed triangular-shaped resonators create two controllable transmission zeros to suppress spurious responses and obtain good skirt rate. The good measured results confirm effectiveness of the proposed filter structure.

2. RESONATOR WITH TWO TRANSMISSION ZEROS

2.1. Resonant Frequencies and Transmission Zeros

The conventional hairpin-line bandpass filter is based on parallel-coupled lines with both ends folded for circuit miniaturization as Fig. 1(a) shows. Since its resonators are $\lambda_g/2$ in length, where λ_g is the guided wavelength, the spurious responses at nf_0 are unavoidable. Fig. 1(b) shows the proposed bandpass filter, consisting of three coupled triangular stepped-impedance resonators, where the resonators are vertically offset from one another, but their wide sides are aligned along a line. The triangular resonators create two tunable transmission zeros to suppress spurious responses and improve skirt rate. Fig. 2(a) shows the schematic of a triangular stepped-impedance resonator (TSIR) which has a triangular shape but is disconnected in the bottom section. If the resonator has uniform impedance ($W_a = W_b$), the electrical length will be $\lambda_g/2$ for resonance. The end-coupled arms of the resonators are not only for increasing loading capacitance, but also for creating two tunable transmission zeros.

Figure 2(b) shows the equivalent transmission line model, in which TSIRs can be modeled using parallel connections of a transmission line with (Z_a, $2\theta_a$) and two lines (Z_b, θ_b) having an end-coupled capacitance C_1 in between. Notably, C_2 denotes the coupling capacitance of input/output ports. Since the resonator structure is symmetric, it can support both even and odd modes. The first odd-mode resonates at f_0 (operating frequency), and the first even-mode resonates at f_1 (first spurious frequency), and so forth. At f_{z1}, the split bottom line of resonators is a quarter-wave open stub such that the feeding point is virtually short-circuited. The existence of C_1 creates more than one signal path between input and output ports as noted by dotted lines. When the two paths are exactly 180° out of phase, the second

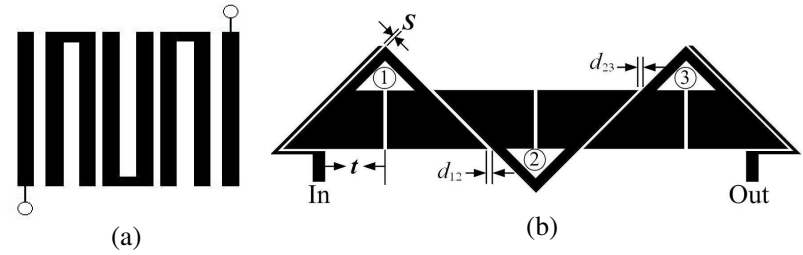

Figure 1. (a) Conventional third-order hairpin-line bandpass filter. (b) Proposed spurious suppressed bandpass filter with triangular stepped-impedance resonators.

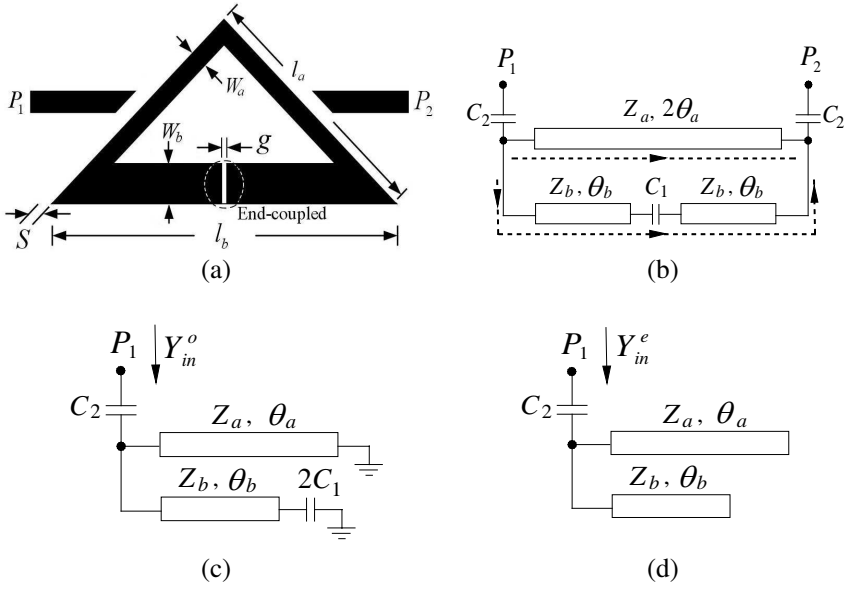

Figure 2. (a) Schematic of the triangular stepped-impedance resonator. (b) Equivalent transmission line model. (c) Odd-mode equivalent circuit. (d) Even-mode equivalent circuit.

transmission zero f_{z2} occurs. Thus, the proposed resonator creates two transmission zeros.

To analyze design parameters of resonators, the odd- and even-mode equivalent circuits can be applied as shown in Figs. 2(c) and

2(d). The odd-mode input admittance seen from P_1 of Fig. 2(c) is

$$Y_{in}^{o} = j\frac{\omega C_2[Z_a(2\omega C_1 Z_b + \tan\theta_b) + Z_b\cot\theta_a(2\omega C_1 Z_b\tan\theta_b - 1)]}{Z_a(2\omega C_1 Z_b + \tan\theta_b) + Z_b(2\omega C_1 Z_b\tan\theta_b - 1)(\cot\theta_a - \omega C_2 Z_a)}. \quad (1)$$

When $Y_{in}^{o} = 0$, odd-mode resonance will occur, and the resonant condition is

$$Z_a(2\omega C_1 Z_b + \tan\theta_b) + Z_b\cot\theta_a(2\omega C_1 Z_b\tan\theta_b - 1) = 0. \quad (2)$$

Similarly, the even-mode input admittance in Fig. 2(d) is derived as

$$Y_{in}^{e} = j\frac{\omega C_2(Z_a\tan\theta_b + Z_b\tan\theta_a)}{(Z_a\tan\theta_b + Z_b\tan\theta_a + \omega C_2 Z_a Z_b)}. \quad (3)$$

Even-mode resonance can be formulated with $Y_{in}^{e} = 0$, which is

$$Z_a\tan\theta_b + Z_b\tan\theta_a = 0. \quad (4)$$

The transmission zero occurs when $S_{21} = 0$. The S_{21} parameter can be derived with the odd- and even-mode input admittances, and is given by

$$S_{21} = \frac{Y_{in}^{o}Y_o - Y_{in}^{e}Y_o}{(Y_o + Y_{in}^{o})(Y_o + Y_{in}^{e})} = 0, \quad (5)$$

where Y_o is the characteristic admittance. From (5), it is found that $Y_{in}^{o} = Y_{in}^{e}$, which gives the condition of transmission zeros:

$$\omega C_1(Z_a\sin 2\theta_a + Z_b\sin 2\theta_b) - \cos^2\theta_b = 0. \quad (6)$$

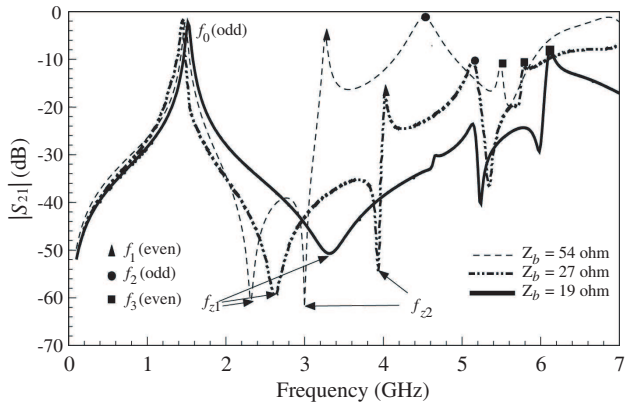

Figure 3. Simulated $|S_{21}|$ responses of a single triangular stepped-impedance resonator with various Z_b ($Z_a = 54\,\Omega$, $\theta_a = 63.3°$, $\theta_b = 90.3°$, and $g = 0.2\,\text{mm}$).

2.2. Frequency Shift of Spurious Responses and Transmission Zeros

Since the goal of this paper is to obtain a wide stop band, the current study analyzes the frequency variation of spurious responses and transmission zeros of resonators in detail. Observations show that the impedance Z_b of the bottom side of resonators has the most significant affection on frequency shift. When Z_b is decreased (W_b increased), the effective θ_b becomes shorter since l_b is tapered from outside edge to inside edge, which raises the resonant frequency. The odd mode currents concentrate at the vertical angle of resonators, so that f_2 is slightly altered by the decrease of Z_b. On the other hand, the currents of the even mode and the second zero highly concentrate on the two base angles of resonators. Accordingly, f_1 and f_{z2} increase more rapidly as Z_b is decreased. Varying Z_b can shift f_1 and f_{z2} to merge with f_2 to suppress the spurious responses.

Figure 3 compares the simulated $|S_{21}|$ responses of a single triangular stepped-impedance resonator with $Z_b = 54$, 27, and 19 Ω The center frequency is designed at $f_o = 1.5$ GHz. The circuit dimensions are $Z_a = 54\,\Omega$, $\theta_a = 63.3°$, $\theta_b = 90.3°$, and $g = 0.2$ mm, with the substrate parameters of $\varepsilon_r = 10.2$, $\tan\delta = 0.0025$, and $h = 1.27$ mm. Notably, the gap g must be small enough to induce enough C_1 and to cause f_{z2}. The calculated resonant frequencies and transmission zeros from (2), (4), and (6) are checked with the simulated results of Fig. 3, and both have good agreement. As Fig. 3 shows, the frequencies of f_{z2}, f_1, and f_2 increase as Z_b decreases, in which their change rates have a relation of $f_{z2} > f_1 > f_2$. Varying Z_b allows f_{z2} to merge with f_1 and f_2 to suppress the leading two spurious responses, as the solid curve of Fig. 3 shows. Moreover, f_{z1} can be used to improve attenuation skirt rate in the upper stopband. Observations also show that f_0 has only a slight frequency shift when Z_b is changed. For spurious suppression, the circuit dimensions of TSIRs are determined as $W_a = 1$, $l_a = 13.6$, $W_b = 5.5$, $l_b = 19.4$, and $g = 0.2$ (all in mm).

3. FILTER SYNTHESIS WITH DIRECT-COUPLED-RESONATOR STRUCTURE

The proposed spurious-suppressed TSIRs are implemented for the bandpass filter design based on the direct-coupled-resonator structure. Fig. 1(b) shows that the three-pole experimental filter consists of three offset triangular stepped-impedance resonators, using the line-to-loop strong coupling for input/output ports. Fig. 4 depicts the equivalent circuit of the filter, where $(LC)^{-1/2} = \omega_o$ is the resonant angular

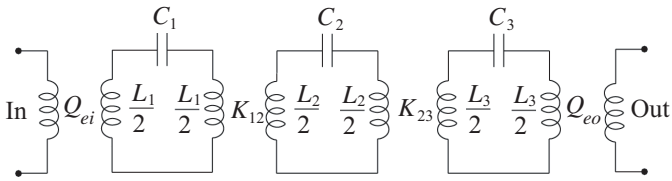

Figure 4. Equivalent circuit of Fig. 1(b) with coupling coefficients K_{ij} and external quality factors Q_e.

frequency. The coefficients K_{ij} specify the coupling between adjacent resonators i and j of the filter, and Q_{ei} and Q_{eo} are the external quality factors that specify the input and output couplings, respectively.

K_{ij} and Q_e can be derived from the associated low-pass prototype of Fig. 4, which is given by

$$K_{ij} = \frac{FBW}{\sqrt{g_i g_j}} \tag{7a}$$

$$Q_{ei} = \frac{g_0 g_1}{FBW} \tag{7b}$$

$$Q_{eo} = \frac{g_N g_{N+1}}{FBW} \tag{7c}$$

where g_i are element values of the lowpass prototype filter and FBW represents the fractional bandwidth of bandpass filters.

When the filter is designed with third-order ($N = 3$), Chebyshev response, and 0.5 dB ripple level, the element values of the low-pass prototype are $g_0 = g_4 = 1$, $g_1 = g_3 = 1.5963$ and $g_2 = 1.0967$. If $f_0 = 1.5$ GHz and $FBW = 8\%$ are required, then $Q_{ei} = Q_{eo} = 19.9537$ and the coupling matrix is

$$[K] = \begin{bmatrix} 0 & 0.06046 & 0 \\ 0.06046 & 0 & 0.06046 \\ 0 & 0.06046 & 0 \end{bmatrix} \tag{8}$$

The design curves of coupling coefficients and external quality factors need to be plotted for determining circuit dimensions. The coupling coefficient between resonators i and j can be calculated using the equation $K_{ij} = \pm \left(f_{p2}^2 - f_{p1}^2\right) / \left(f_{p2}^2 + f_{p1}^2\right)$, where f_{p1} and f_{p2} represent the two simulated split resonant frequencies of a pair of coupled resonators [6]. The external quality factor can be obtained from $Q_e = f_0/\Delta f_{3\,\mathrm{dB}}$, where $\Delta f_{3\,\mathrm{dB}}$ is the 3-dB bandwidth of a singly loaded TSIR. Fig. 5(a) plots the coupling coefficient K as a function of the gap d between the two resonators. From Fig. 5(a), both d_{12} and d_{23} in Fig. 1(a) are set to $d_{12} = d_{23} = 0.28$ mm to yield a coupling

coefficient of 0.06046. Fig. 5(b) plots the design curve of the external quality factor Q_e versus the feeding position t with $S = 0.2$. Generally, a smaller gap S results in a stronger I/O coupling or a smaller external quality factor of the resonator [6]. For providing the proper Q_e, the gap S is chosen to be 0.2 mm. From Fig. 5(b), t in Fig. 1(a) is found to be 5.75 mm with $S = 0.2$, yielding the external quality factor of 19.9537.

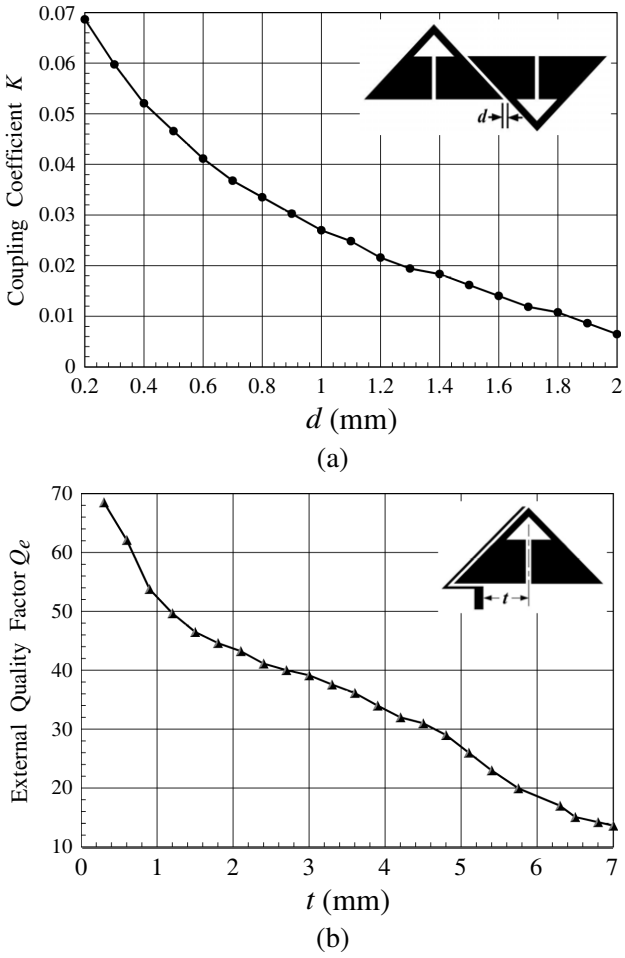

Figure 5. (a) Coupling coefficient K between coupled resonators versus gap d. (b) External quality factor Q_e versus feeding position t with coupled input.

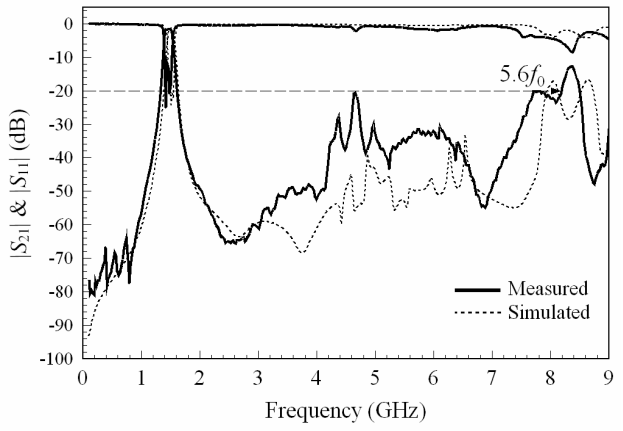

(a)

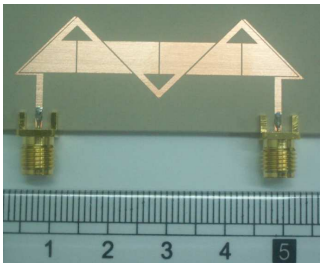

(b)

Figure 6. (a) Measured and simulated responses of the experimental filter. (b) Photograph of the fabricated filter.

4. EXPERIMENTAL RESULTS

The current investigation uses the substrate RT/Duroid 6010 with dielectric constant $\varepsilon_r = 10.2$, $\tan\delta = 0.0025$, and thickness $h = 1.27$ mm for filter fabrication, and the full wave EM software IE3D for simulation. Fig. 6(a) plots the simulated and measured results, and both responses agree closely. The measured center frequency is slightly shifted to 1.51 GHz, showing that the spurious responses are suppressed up to $5.6f_0$ with a rejection level of better than 20 dB. The measured insertion loss, return loss, and 3-dB bandwidth are 1.55 dB, 18.7 dB, and 8.1%, respectively. Fig. 6(b) displays a photograph of the fabricated filter.

5. CONCLUSION

A novel spurious suppressed bandpass filter based on the direct-coupled-resonator configuration with stepped-impedance resonators is presented. The proposed triangular-shaped stepped-impedance resonators create two tunable transmission zeros which are applied to suppress multi spurious responses and achieve sharp skirt selectivity. The frequency shift of spurious responses and transmission zeros due to the dimension variation of resonators is investigated. Design curves of the coupling coefficients and external quality factors are plotted for filter synthesis. This work designed and fabricated an experimental third-order Chebyshev bandpass filter operating at 1.5 GHz. The measured responses with suppression of over 20 dB and up to $5.6f_0$ validate effectiveness of the proposed circuit structure.

ACKNOWLEDGMENT

This work was partially supported by the National Science Council, Taiwan, R.O.C., (NSC 97-2221-E-182-015) and Chang Gung University, Taiwan, R.O.C., (UERPD280061). We would also like to recognize the support of the High Speed Intelligent Communication (HSIC) Research Center, Chang Gung University.

REFERENCES

1. Cristal, E. G. and S. Frankel, "Hairpin-line and hybrid hairpin-line half-wave parallel-coupled-line filters," *IEEE Trans. Microwave Theory Tech.*, Vol. 20, 719–728, Nov. 1972.
2. Sagawa, M., K. Takahashi, and M. Makimoto, "Miniaturized hairpin resonator filters and their application to receiver front-end MIC's," *IEEE Trans. Microwave Theory Tech.*, Vol. 37, 1991–1996, Dec. 1989.
3. Ma, K., K. S. Yeo, J. Ma, and M. A. Do, "An ultra-compact hairpin band pass filter with additional zero points," *IEEE Microwave and Wireless Components Letters*, Vol. 17, 262–264, Apr. 2007.
4. Adam, H., A. Ismail, M. A. Mahdi, M. S. Razalli, A. R. H. Alhawari, and B. K. Esfeh, "X-band miniaturized wideband bandpass filter utilizing multilayered microstrip hairpin resonator," *Progress In Electromagnetics Research*, PIER 93, 177–188, 2009.
5. Lee, S.-Y. and C.-M. Tsai, "New cross-coupled filter design using

improved hairpin resonators," *IEEE Trans. Microwave Theory Tech.*, Vol. 48, 2482–2490, Dec. 2000.

6. Hong, J. S. and M. J. Lancaster, *Microstrip Filters for RF/Microwave Applications*, John Wiley & Sons Inc., 2001.
7. Hong, J. S. and M. J. Lancaster, "Theory and experiment of novel microstrip slow-wave open-loop resonator filters," *IEEE Trans. Microwave Theory Tech.*, Vol. 45, 2358–2365, Dec. 1997.
8. Velázquez-Ahumada, M. C., J. Martel, and F. Medina, "Parallel coupled microstrip filters with ground-plane aperture for spurious band suppression and enhanced coupling," *IEEE Trans. Microwave Theory Tech.*, Vol. 52, 1082–1086, Mar. 2004.
9. Tu, W.-H. and K. Chang, "Compact microstrip bandstop filter using open stub and spurline," *IEEE Microwave and Wireless Component Letters*, Vol. 15, 268–270, Apr. 2005.
10. Wu, C.-H., Y.-S. Lin, C.-H. Wang, and C.-H. Chen, "A compact LTCC ultra-wideband bandpass filter using semi-lumped parallel-resonance circuits for spurious suppression," *European Microwave Conference 2007*, 532–535, Munich, Germany, Oct. 9–12, 2007.
11. Wang, C.-H., P.-H. Deng, and C.-H. Chen, "Coplanar-waveguide-fed microstrip bandpass filters with capacitively broadside-coupled structures for multiple spurious suppression," *IEEE Trans. Microwave Theory Tech.*, Vol. 55, 768–775, Apr. 2007.
12. Chin, K.-S., Y.-C. Chiang, and J.-T. Kuo, "Microstrip open-loop resonator with multi-spurious suppression," *IEEE Microwave and Wireless Components Letters*, Vol. 17, 574–576, Aug. 2007.
13. Chaimool, S., S. Kerdsumang, and P. Akkaraekthalin, "A novel microstrip bandpass filter using triangular open-loop resonators," *Asia-Pacific Conference on Communications 2003*, 788–791, Sept. 21–24, 2003.
14. Görür, A. and C. Karpuz, "Cross-coupled bandpass filter using microstrip triangular open-loop resonators," *European Microwave Conference 2001*, 1–4, London, England, Oct. 2001.
15. Zhang, J., J.-Z. Gu, B. Cui, and X.-W. Sun, "Compact and harmonic suppression open-loop resonator bandpass filter with tri-section SIR," *Progress In Electromagnetics Research*, PIER 69, 93–100, 2007.